Journal of Power Sources 196 (2011) 10479–10483

Contents lists available at ScienceDirect

Journal of Power Sources

journal homepage: www.elsevier.com/locate/jpowsour

Short communication

Development of all-solid-state mediator-enhanced supercapacitors with polyvinylidene fluoride/lithium trifluoromethanesulfonate separators

Juanjuan Zhou[a,*], Jinshu Cai[a], Sirui Cai[a], Xiangyang Zhou[a], Azzam N. Mansour[b]

[a] Department of Mechanical and Aerospace Engineering, University of Miami, Coral Gables, FL 33124, United States
[b] Materials and Power Systems Branch, Carderock Division, NSWC, West Bethesda, MD 20817, United States

ARTICLE INFO

Article history:
Received 9 August 2011
Accepted 9 August 2011
Available online 17 August 2011

Keywords:
PVDF
Solid-state
Supercapacitor
Mediator

ABSTRACT

All-solid-state supercapacitors (SCs) were fabricated using a polyvinylidene fluoride (PVDF)/lithium trifluoromethanesulfonate (LiTFS) membrane as the separator and poly(ethylene oxide) (PEO)/lithium perchlorate ($LiClO_4$) as the polymer electrolyte in the porous carbon electrodes. Two types of mediators, NaI/I_2 and $K_3Fe(CN)_6/K_4Fe(CN)_6$, were added into the $PEO/LiClO_4$ polymer electrolyte that was used to fabricate the electrodes. The voltage window in which the SCs operated was 2.5–3 V. The results of electrochemical measurements, including cyclic voltammetry and galvanostatic charge/discharge, indicated that NaI/I_2-containing and $K_3Fe(CN)_6/K_4Fe(CN)_6$-containing SCs yielded high specific capacitances of 209.0 and 138.8 $F\,g^{-1}$, respectively. In addition to high specific capacitances for the two mediator-containing SCs, both SCs delivered high specific energies (49.1 $Wh\,kg^{-1}$ at 1.6 $kW\,kg^{-1}$ for the NaI/I_2-containing SC and 33.6 $Wh\,kg^{-1}$ at 1.3 $kW\,kg^{-1}$ for the $K_3Fe(CN)_6/K_4Fe(CN)_6$-containing SC) due to the wide voltage window and fast redox reactions between mediators.

1. Introduction

With higher specific power than batteries and higher specific energy than dielectric capacitors, supercapacitors (SCs) are able to fill the gap between these two devices. Recent attention directed at SCs has been stimulated by their potential applications in energy storage devices, power electronics, and hybrid electric vehicles.

Traditionally, SCs are categorized into three groups depending on the active materials in their electrodes: carbon or electrochemical double layer (EDL) [1,2], metal oxide [3,4], and conducting polymer SCs [5,6]. The capacitance of carbon-based SCs is realized through the separation of electrons and ionic charges at the interface between carbon with a large surface-area and electrolytes [7]. In the metal oxide and conducting polymer-based SCs, fast Faradaic reactions, which are also known as a redox or pseudocapacitive process, take place between active electrode materials [8]. In addition, hybrid SCs based on a combination of carbon and conducting polymers, and a combination of carbon and metal oxides have been recently developed [9,10]. Generally speaking, SCs based on redox reactions or pseudocapacitance have greater specific energies than EDL SCs. The high specific power of an SC relies on the high ionic conductivity of the electrolytes, particularly aqueous electrolytes [11,12]. However, the voltage window of aqueous or water-related electrolytes is limited to 0.0–1.0 V because of the electrolysis of water. As a result, higher valences of the active materials cannot be utilized, and the energy density is limited. To address this issue, researchers have used organic electrolytes or ionic liquids to replace aqueous electrolytes to obtain a greater voltage window [13]. However, SCs based on liquid electrolytes suffer from the following problems: inherent leakage, corrosion or combustion, narrow temperature range, inflexible geometry, and poor safety. Although all-solid-state SCs are free of these problems, they are generally not as good as the liquid electrolyte SCs in terms of specific capacitance, specific energy, and specific power, even though the same active materials are used [14–17]. The major reasons for this may be the relatively low ionic conductivity and insufficient viscosity or fluidity of solid electrolytes. For example, at room temperature, commonly used 1 $mol\,dm^{-3}$ H_2SO_4 solution has an ionic conductivity of 0.8 $S\,cm^{-1}$, whereas the fully hydrated Nafion membrane has an ionic conductivity of only 0.2 $S\,cm^{-1}$ and the conductivity of lithium-ion-conducting polymer electrolytes is even lower, at 10^{-5} to 10^{-3} $S\,cm^{-1}$ [18,19]. Insufficient fluidity may result in inadequate contact between the active materials and solid electrolyte, thereby making it difficult for ions to access the active materials in the small pores of a porous electrode. The accessibility of the ions to the active materials is important because the formation of a layer with an opposite charge is required to maintain electroneutrality in charged electrodes.

In dye-sensitized solar cells, mediators, including I^-/I_3^-, Co(III)/Co(II) complexes and ferrocene/ferrocenium among others,

* Corresponding author. Tel.: +1 305 284 2579; fax: +1 305 284 2580.
E-mail address: j.zhou9@umiami.edu (J. Zhou).

0378-7753/$ – see front matter © 2011 Elsevier B.V. All rights reserved.
doi:10.1016/j.jpowsour.2011.08.051

Table 1
Contents of the three types of electrode suspensions.

Suspension name	Composition (wt%)						
	PEO	$LiClO_4$	CB	NaI	I_2	$K_4Fe(CN)_6$	$K_3Fe(CN)_6$
Carbon black	61.4	18.6	20.0	0	0	0	0
NaI/I_2/CB	61.4	18.6	2.0	6.7	11.3	0	0
$K_4Fe(CN)_6$/$K_3Fe(CN)_6$/CB	61.4	18.6	2.0	0	0	9.5	8.5

have been used to enable both electron transport in the electrolyte and electron transfer at the electrode/electrolyte interface [20–23]. Mediators that can undergo redox reactions can be uniformly distributed in the electrolytes in the form of discrete molecules or molecular clusters. Thus, all mediator molecules are theoretically accessible to the ions contained in the solid electrolyte. Other benefits of using mediators as the active materials instead of metal oxides or electronically conducting polymers are as follows. First, pseudocapacitance is provided via the redox reactions of the mediators. Second, the conductivity of the electrolyte in the porous electrodes can be increased via fast electron transfer between mediators. Third, mediators such as NaI and I_2 can be acquired at a much lower cost than noble metal oxides.

In previous studies on all-solid-state mediator SCs by the present authors, Nafion membranes were used as the separator, and a PEO polymer electrolyte doped with NaI/I_2 mediators was used to fabricate the electrodes [24,25]. Previous results have shown that SCs prepared using this novel method can achieve high specific capacitance, high specific power, high specific energy, long cycle life, and low self-discharge. This demonstrates that in addition to carbon materials, metal oxides, and electronically conducting polymers, mediator-doped polymer electrolytes are a fourth type of material that can be utilized to fabricate all-solid-state SCs. The reasons that a Nafion membrane was chosen to be the separator are its low resistance, good mechanical strength, thermal stability, and chemical stability. However, the voltage window for Nafion-based SCs is between 0.0 and 1.0 V or between −1.0 and 0.0 V, which limits full utilization of the high valence states of the active materials. Thus, in the present work, a PVDF/LiTFS membrane was made to replace the Nafion membrane as the separator. Because the membrane and the mediator-doped PEO electrolytes did not contain water, it was envisioned that the voltage window could be greater than 1.0 V. The performance of the SC was evaluated using cyclic voltammetry (CV) and galvanostatic charge/discharge (GCD) methods. The main objective was to demonstrate that with a PVDF/LiTFS membrane as the separator, a high performance all-solid-state SC could be realized.

2. Experimental

2.1. Preparation

2.1.1. Preparation of PVDF/LiTFS membrane

PVDF powder (M.W. = 534,000, Sigma–Aldrich) was mixed with LiTFS powder (~99.995%, Sigma–Aldrich). The mixture was dissolved in acetone (99.9%, Sigma–Aldrich) and then stirred at 60 °C for approximately 4 h until the suspension became a homogeneous translucent gel. The mass ratio of PVDF to LiTFS was 1:1. The gel was cast into evaporation dishes and allowed to dry for 12 h to obtain a thin, transparent PVDF/LiTFS membrane.

2.1.2. Preparation of PEO-based suspensions for electrode loadings

A mixture of PEO (M.W. = 400,000, Sigma–Aldrich) and $LiClO_4$ (≥98%, Fluka) was dissolved in acetonitrile (Sigma–Aldrich) and then stirred at 60 °C for approximately 4 h until the suspension became a homogeneous translucent gel. The molar ratio of PEO monomer to $LiClO_4$ in the gel was 8:1. Sodium iodide (NaI, 99.55%, Alfa Aesar), iodine (I_2, 99.8%, Alfa Aesar), potassium hexacyanoferrate ($K_4Fe(CN)_6{\cdot}H_2O$, 98.5–102.0%, Sigma–Aldrich), potassium ferricyanide ($K_3Fe(CN)_6$, 99%, Sigma–Aldrich), and carbon black (VULCAN XC72R) were added into the PEO/$LiClO_4$ gel separately to form the electrode suspensions. Three types of electrode suspensions were prepared, namely, the carbon black (CB) suspension, the NaI/I_2/CB suspension, and the $K_3Fe(CN)_6$/$K_4Fe(CN)_6$/CB suspension. The contents of the three kinds of suspensions are listed in Table 1.

2.1.3. Preparation of supercapacitor assemblies

A nanofoam carbon paper was acquired from Marketech International Inc. The specification of the carbon paper is as follows: density, 0.25–1.0 g cm^{-3}; BET surface area, 400 m^2 g^{-1}; average pore size, 0.7 nm; electrical resistivity, 0.010–0.040 Ω cm. The prepared PEO-based suspension was dropped on a piece of nanofoam carbon paper. After loading with suspensions, the electrodes were dried naturally in air for approximately 12 h and then kept in a plastic bag.

To make an SC assembly, the PVDF membrane prepared in Section 2.1.1 was used as the separator. Two carbon electrodes (1.0 cm^2) loaded with active materials and polymer electrolytes, and a PVDF membrane were pressed at approximately 1000 psi for 1 min to obtain a sandwich structured SC, as shown in Fig. 1.

2.2. Characterization

Electrochemical impedance spectroscopy (EIS), cyclic voltammetry (CV), and galvanostatic charge/discharge (GCD) measurements were conducted at ambient temperature using solid-state electrochemical cells or SC assemblies in the form shown in Fig. 1. The SC was connected to a potentiostat (Gamry) with a frequency response analyzer module interfaced to a personal computer. For the EIS measurements, the applied frequency range was between 1 Hz and 100 kHz, and the amplitude of the sinusoidal voltage was 10 mV. The performance of the SCs was studied using CV (voltage range of 0.0–3.0 V, scanning rate of 10–200 mV s^{-1}) and GCD (charge/discharge current density of 10–25 mA cm^{-2}).

In addition to the EIS measurements on the SC assembly, the lateral or in-plane conductivities of the PVDF/LiTFS and Nafion films were evaluated using a four-electrode AC impedance method described in detail in a previous publication [26].

3. Results and discussion

3.1.1. Conductivity analysis of the PVDF/LiTFS membrane

The conductivity of the membrane separator in a solid-state SC is crucial to its performance. Therefore, the conductivity of the PVDF/LiTFS membrane was tested using the four-electrode method [26]. In addition, for comparison, the conductivity of a commercial Nafion® 117 membrane was also evaluated with the same method, and the data are given in Table 2. Before conducting the conductivity measurement with the Nafion membrane, it was fully hydrated and activated in 1 mol dm^{-3} sulfuric acid for 12 h.

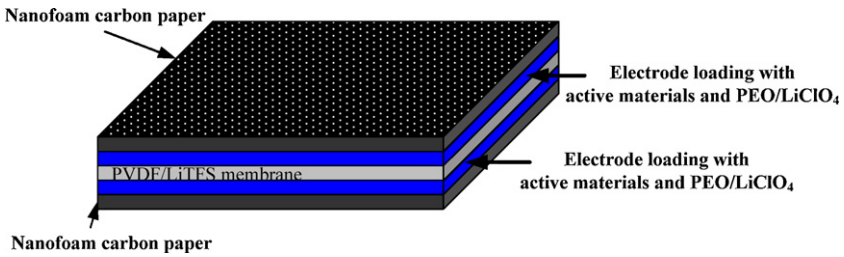

Fig. 1. Schematic of an all-solid-state supercapacitor assembly.

Table 2
Conductivity of PVDF/LiTFS and Nafion 117 membranes under ambient conditions.

Membrane	Conductivity, S cm^{-1}	Average conductivity, S cm^{-1}
PVDF/LiTFS	1.730×10^{-2} 1.747×10^{-2} 1.745×10^{-2}	1.74×10^{-2}
Nafion 117	2.715×10^{-2} 2.734×10^{-2} 3.041×10^{-2}	2.83×10^{-2}

As shown in Table 2, the average conductivity values for the PVDF/LiTFS and Nafion membranes are 1.74×10^{-2} and 2.83×10^{-2} S cm^{-1} at 25 °C, respectively. The conductivity of the PVDF/LiTFS membrane is lower than that of a fully hydrated Nafion membrane. However, the relatively high conductivity and stability of the PVDF/LiTFS membrane have made them outstanding among the currently studied lithium-ion-conducting polymer membranes [27,28]. On the other hand, the ionic conduction in Nafion membranes depends on the hydration level, which means that if it is dehydrated under ambient conditions, the conductivity will decrease [29]. The ionic conduction in polymers containing lithium ions is believed to rely on the diffusion of lithium ions, which have a small ionic radius, through the free volume in the polymer [30]. This implies that with a PVDF/LiTFS membrane, a high ionic conductivity can be obtained without the presence of water in the polymer.

3.2. Cyclic voltammetry

3.2.1. Supercapacitors with carbon black

To establish a reference for evaluating the effects of the two kinds of mediators, an all-solid-state SC that contained only carbon black as the active material was assembled, and its performance was evaluated using cyclic voltammetry. Fig. 2 illustrates the cyclic voltammograms of a carbon black SC at different scanning rates. No redox peaks were observed in the CVs of the carbon SC, indicating that this kind of SC is a typical EDL SC. Fig. 2 also shows that the current density increased as the scanning rate decreased. It is widely accepted that the CV of an ideal EDL SC is rectangular-shaped. However, for the carbon black SC in the present configuration, the CVs at different scanning rates were not rectangular-shaped, showing poor reversibility [31]. This poor reversibility may result from a high series resistance (10.9 Ω) of the carbon black SC.

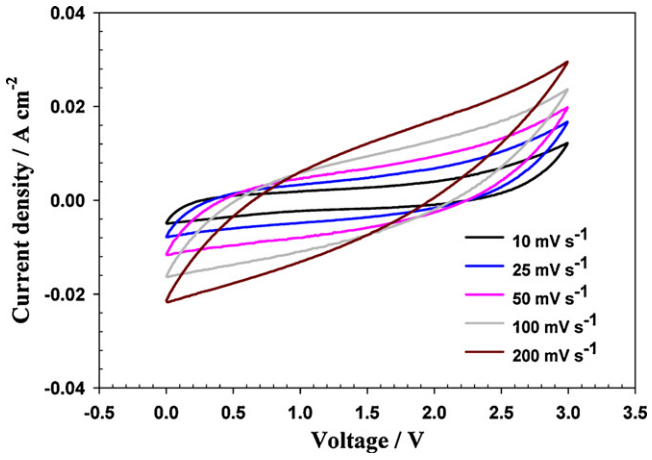

Fig. 2. Cyclic voltammetry curves as a function of potential scanning rate for a supercapacitor with carbon black as the active material.

According to the CV results, the specific capacitance with respect to the active material is calculated using the following equation [31]:

$$C_{active} = \frac{Min(q_a, q_c)}{\Delta V \cdot m_{active}} \quad (1)$$

where q_a and q_c are the sums of charge calculated for the anodic and cathodic polarization half cycles, respectively, ΔV is the voltage window of the CV test (3 V), and m_{active} is the total mass of active materials (carbon black for the activated carbon SC and carbon black plus mediators for the mediator enhanced SCs). The specific capacitance values are listed in Table 3. According to Table 3, the specific capacitance of the carbon black SC was 40.7 F g^{-1} at a scanning rate of 10 mV s^{-1}, and the capacitance decreased upon increasing the scanning rate.

3.2.2. Supercapacitors with sodium iodide/iodine (NaI/I_2) mediators

Fig. 3 shows CV curves for a NaI/I_2-containing SC at scanning rates from 10 to 200 mV s^{-1}. All of the CVs showed a slightly distorted rectangular shape without distinct, sharp redox peaks [32]. In addition, both the absence of sharp redox peaks and the presence of high current density compared to that of the carbon black SC are characteristic features of electrochemical materials with pseudocapacitance [33,34]. The specific capacitance was 209.0 F g^{-1} at a scanning rate of 10 mV s^{-1}. The specific capacitances of the NaI/I_2-containing SC were 5–10 times greater than those of the carbon black SC depending on the scanning rate, showing an enhancement effect of the NaI/I_2 mediators due to the pseudocapacitance. Moreover, with the NaI/I_2-containing SC, the changes of current polarity when the voltage scan was reversed were much faster than those of the carbon black SCs, indicating a lower internal resistance and good reversibility [35]. This was confirmed by the EIS results (data not shown), which showed that the internal resistance was only

Table 3
Summary of the specific capacitance of the carbon black SC, the NaI/I_2/CB SC, and the $K_4Fe(CN)_6/K_3Fe(CN)_6$/CB SCs.

Scanning rate, mV s^{-1}	Specific capacitance, F g^{-1}		
	Carbon black	NaI/I_2/CB	$K_4Fe(CN)_6/K_3Fe(CN)_6$/CB
10	40.7	209.0	138.8
25	20.4	145.4	99.8
50	10.2	107.5	82.5
100	7.9	89.0	50.4
200	5.8	52.9	36.5

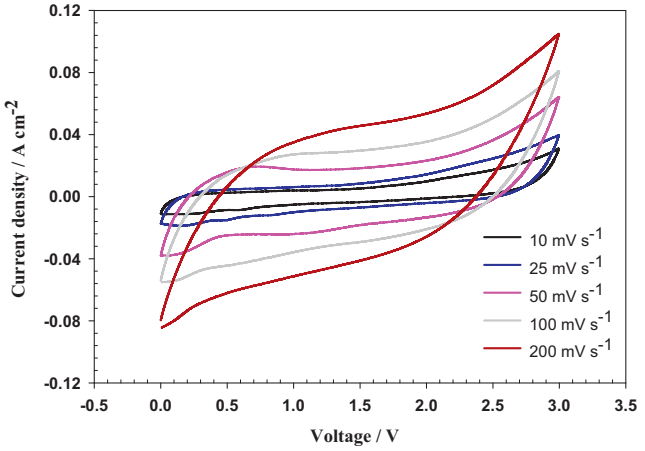

Fig. 3. Cyclic voltammetry curves as a function of potential scanning rate for a supercapacitor with NaI/I_2/CB as the active material.

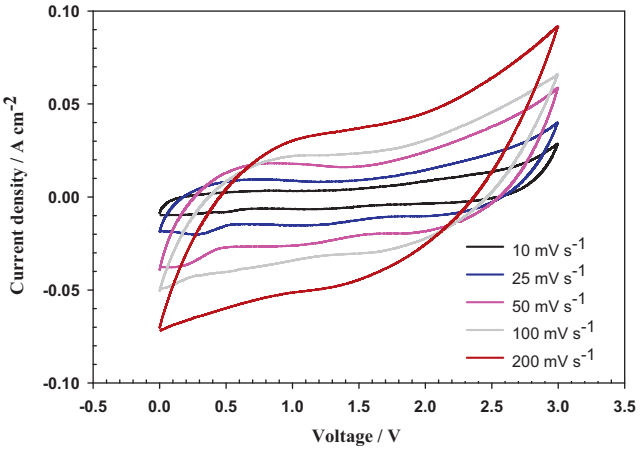

Fig. 4. Cyclic voltammetry curves as a function of potential scanning rate for a supercapacitor with $K_3Fe(CN)_6/K_4Fe(CN)_6$/CB as the active material.

3.6 Ω. In this system, the mediators behave as both conducting charge carriers and charge storage materials. In fact, in contributing to those properties, two elemental processes are involved in the mediator-related conduction process of an electrode containing both a polymer electrolyte and mediators: (1) physical migration of the ionic species (Na^+ and I^-), and (2) electron transfer reactions that cause a net charge displacement. The latter exists only in the presence of the mediators, where fast electron exchange occurs between mediators. A detailed description of the enhancement effect on the conductivity with the addition of mediators can be found in a previous publication [24]. According to the discussion in Ref. [24], the pseudocapacitance of the NaI/I_2-containing SC originates from the following redox reactions: $I_2(s) + 2e^- = 2I^-$ and $I_3^- + 2e^- = 3I^-$. However, for the SC with NaI/I_2 mediators, no sharp redox peaks were observed in the CV results, revealing a typical capacitive behavior that can be found in other systems with pseudocapacitance [3–6]. The addition of mediators increases the capacitance by contributing pseudocapacitance, which is a dominant component in the overall capacitance. Moreover, it can also be concluded from Fig. 3 that the current density increased proportionally with the scanning rate, which is also considered as a typical characteristic of an EDL SC [36].

3.2.3. Supercapacitor with $K_3Fe(CN)_6/K_4Fe(CN)_6$ mediators

$K_3Fe(CN)_6$ and $K_4Fe(CN)_6$ are known to engage in fast electron transfer between themselves [33]. The carbon nanofoam electrodes employed contained PEO/$LiClO_4$, $K_3Fe(CN)_6/K_4Fe(CN)_6$, and carbon black. Fig. 4 shows CV curves at scanning rates from 10 to 200 mV s^{-1}. The shapes of the CV curves for the $K_3Fe(CN)_6/K_4Fe(CN)_6$-containing SC were similar to those observed for the NaI/I_2-containing SC and other systems with pure capacitive behavior. However, a pair of broad redox peaks appeared at approximately 0.5 V. The redox peaks are believed to be related to the redox reaction $K_3Fe(CN)_6 + e^- + K^+ = K_4Fe(CN)_6$ [37].

The specific capacitance of the $K_3Fe(CN)_6/K_4Fe(CN)_6$-containing SC as a function of the scanning rate is also listed in Table 3. The specific capacitance was 138.8 F g^{-1} at a scanning rate of 10 mV s^{-1}, which is much less than 209.0 F g^{-1}, the specific capacitance of the NaI/I_2-containing SC at the same scanning rate. It is worth noting that the theoretical specific charge of the $K_3Fe(CN)_6/K_4Fe(CN)_6$ mediators (in a molar ratio of 1:1) is 138.3 C g^{-1}, which is smaller than the theoretical specific charge of 239.1 C g^{-1} for the NaI/I_2 mediators (in a molar ratio of 1:1). The specific capacitance increased as the scanning rate decreased, which is a behavior similar to both the carbon black SC and NaI/I_2-containing SC. However, for this $K_3Fe(CN)_6/K_4Fe(CN)_6$-containing SC, the specific capacitance was 3–6 fold that of the carbon black SC, depending on the scanning rate. Thus, the enhancement effect was not as pronounced as with NaI/I_2 mediators.

3.3. Galvanostatic charge/discharge

Galvanostatic charge/discharge tests were also conducted to evaluate the performance, specifically the specific energy and specific power of SCs with NaI/I_2 and $K_3Fe(CN)_6/K_4Fe(CN)_6$ mediators, and the results are shown in Fig. 5(A) and (B). The tests were conducted in a voltage range between 0.0 and 2.5 V at charge/discharge current densities of 10, 15, 20, and 25 mA cm^{-2}. Fig. 5 shows that

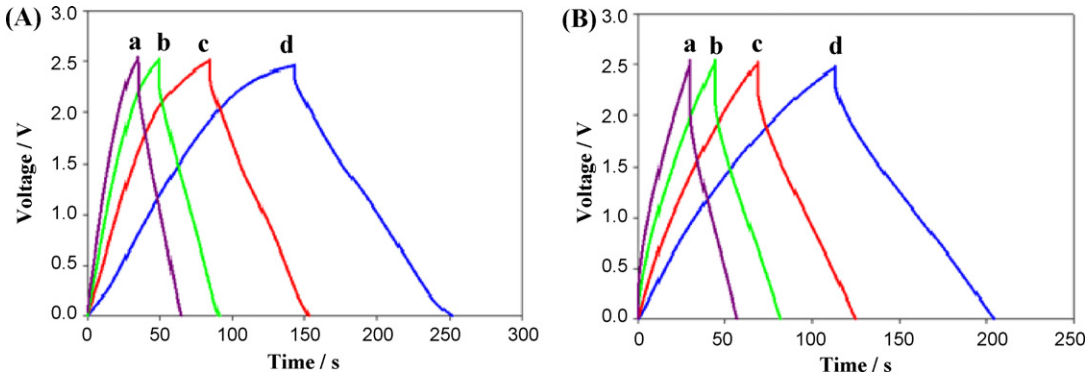

Fig. 5. Representative cell voltage versus time curves for (A) NaI/I_2/CB SC and (B) $K_3Fe(CN)_6/K_4Fe(CN)_6$/CB SC, with constant charge/discharge current densities of (a) 25, (b) 20, (c) 15, and (d) 10 mA cm^{-2}.

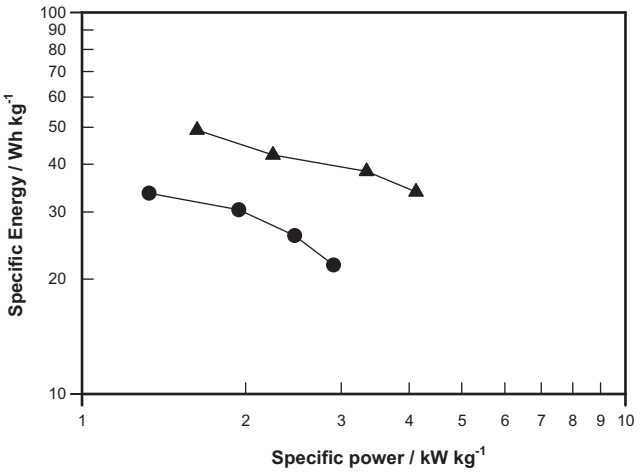

Fig. 6. Ragone plots for a NaI/I_2/CB SC (▲) and a $K_3Fe(CN)_6/K_4Fe(CN)_6$/CB SC (●).

for both SCs, regardless of the value of the charge/discharge current density, the discharge curves were essentially linear over the entire discharge period except for a small sharp drop in the very initial stage, which corresponds to the ohmic loss due to series resistance [38]. The linearity of the discharge curves indicated that the mediator-containing SCs described in this work have typical capacitive characteristics and resemble an EDL SC [39]. Specific energy (SE) and specific power (SP) were also evaluated from the galvanostatic charge/discharge results using the following equations:

$$\mathrm{SE} = \frac{I\int_t^{t+\Delta t} V(t)dt}{m_{active} \times 3600} \quad (2)$$

$$\mathrm{SP} = \frac{\mathrm{SE}}{\Delta t} \quad (3)$$

where I is the discharge current density, $V(t)$ is the voltage as a function of time, Δt is the discharge time, and m_{active} is the mass of the active material. The specific energy values as a function of specific power for both mediator-containing SCs are shown in Fig. 6 in the form of a Ragone plot. In addition to maintaining a greater charge capacity, both mediator SCs could simultaneously deliver a high specific energy and power. The NaI/I_2-containing SC exhibited a better performance in terms of specific energy and specific power than the $K_3Fe(CN)_6/K_4Fe(CN)_6$-containing SC. This is in line with results of the CV tests. The maximum specific energy of the NaI/I_2-containing SC with a PVDF separator was 49.1 Wh kg^{-1} with respect to the mass of active material, which is about 2 times the maximum specific energy of an SC with a Nafion separator and NaI/I_2 mediator [24]. The higher specific energy for SCs with a Nafion separator is mainly due to the greater voltage window for the SC with a PVDF/LiTFS separator compared to SCs with a Nafion separator.

4. Conclusion

1. Membranes composed of PVDF and LiTFS in a weight ratio of 1:1 were prepared, and their conductivity was 1.74×10^{-2} S cm^{-1}. This kind of membrane was then used as the separator in a solid-state mediator SC.
2. With the use of water-free PVDF/LiTFS polymer membranes and $PEO/LiClO_4$ polymer electrolytes, the operating voltage window of mediator SCs can reach 2.5–3 V, resulting in a significant increase of the specific energy compared with mediator SCs with a Nafion separator, for which the operating voltage window is only 1.0 V.
3. Two types of mediators containing NaI/I_2 and $K_3Fe(CN)_6/K_4Fe(CN)_6$ were added into the $PEO/LiClO_4$ polymer electrolyte to improve the performance of the solid-state SC. Compared to 40.7 F g^{-1}, which is the specific capacitance of a carbon black SC at a scanning rate of 10 mV s^{-1}, the specific capacitances of the NaI/I_2-containing and $K_3Fe(CN)_6/K_4Fe(CN)_6$-containing SCs at a scanning rate of 10 mV s^{-1} were 209.0 and 138.8 F g^{-1}, respectively. The enhancement of the performance of the mediator SCs with respect to the carbon black SC is mainly due to an enhancement of the conductivity of the electrolyte in the porous electrodes and the pseudocapacitance provided by the mediators.

Acknowledgements

The authors would like to thank the Office of Naval Research (ONR) for financial support of this research under award numbers N00014-08-1-0332 and N00014-08-WX-20797.

References

[1] C. Portet, P.L. Taberna, P. Simon, E. Flahaut, J. Power Sources 139 (2005) 371–378.
[2] J. Zhao, C. Lai, Y. Dai, J. Xie, Mater. Lett. 61 (2007) 4639–4642.
[3] V. Subramanian, S.C. Hall, P.H. Smith, B. Rambabu, Solid State Ionics 175 (2004) 511–515.
[4] S.G. Kandalkar, J.L. Gunjakar, C.D. Lokhande, Appl. Surf. Sci. 254 (2008) 5540–5544.
[5] G.M. Suppes, B.A. Deore, M.S. Freund, Langmuir (2008) 1064–1069.
[6] F. Cebeci, E. Sezer, A. SezaiSarac, Electrochim. Acta 635 (2009) 4–6360.
[7] R. Amade, E. Jover, B. Caglar, T. Mutlu, E. Bertran, J. Power Sources 196 (2011) 5779–5783.
[8] K.S. Ryu, K.M. Kim, N.-G. Park, Y.J. Park, S.H. Chang, J. Power Sources 103 (2002) 305–309.
[9] J. Jang, J. Bae, M. Choi, S.-H. Yoon, Carbon 43 (2005) 2730–2736.
[10] D.-W. Wang, F. Li, H.-M. Cheng, J. Power Sources 185 (2008) 1563–1568.
[11] K.S. Ryu, Y.G. Lee, K.M. Kim, Y.J. Park, Y.S. Hong, X.L. Wu, M.G. Kang, N.G. Park, R.Y. Song, J.M. Ko, Synth. Met. 153 (2005) 89–92.
[12] J. Wang, Y.L. Xu, X. Chen, X.F. Du, J. Power Sources 163 (2007) 1120–1125.
[13] D. Villers, D. Jobin, C. Soucy, D. Cossement, R. Chahine, L. Breau, D. Bélanger, J. Electrochem. Soc. 150 (2003) A747–A752.
[14] M.J. Bleda-Martinez, J.A. Macia-Agullo, D. Lozano-Castello, E. Morallon, D. Cazorla-Amoros, A. Linares-Solano, Carbon 43 (2005) 2677–2684.
[15] I.H. Kim, J.H. Kim, Y.H. Lee, K.B. Kim, J. Electrochem. Soc. 152 (2005) A2170–A2178.
[16] P. Staiti, F. Lufrano, Electrochim. Acta 53 (2007) 710–719.
[17] K. Park, H. Ahn, Y. Sung, J. Power Sources 109 (2002) 500–506.
[18] M. Verbrugge, E.W. Schneider, R.S. Conell, R. Hill, J. Electrochem. Soc. 139 (1992) 3421–3428.
[19] M. Park, X. Zhang, M. Chung, G.B. Less, A.M. Sastry, J. Power Sources 195 (2010) 7904–7929.
[20] G.P. Kalaignan, Y.S. Kang, J. Photochem. Photobiol. C: Photochem. Rev. 7 (2006) 17–22.
[21] P.J. Cameron, L.M. Peter, S.M. Zakeeruddin, M. Grätzel, Coord. Chem. Rev. 248 (2004) 1447–1453.
[22] H. Nusbaumer, J.E. Moser, S.M. Zakeeruddin, M.K. Nazeeruddin, M. Gratzel, J. Phys. Chem. B 105 (2001) 10461–10464.
[23] A.F. Nogueira, C. Longo, M.A. De Paoli, Coord. Chem. Rev. 248 (2004) 1455–1468.
[24] J. Zhou, Y. Yin, X. Zhou, A.N. Mansour, Electrochem. Solid-state Lett. 14 (2010) A25–A28.
[25] Y. Yin, J. Zhou, A.N. Mansour, X. Zhou, J. Power Sources 196 (2011) 5997–6002.
[26] X. Zhou, J. Weston, E. Chalkova, M.A. Hofmann, C.M. Ambler, H.R. Allcock, A.N. Lvov, Electrochim. Acta 48 (2003) 2173–2180.
[27] M. Armand, Solid State Ionics 9–10 (1983) 745–754.
[28] T. Itoh, M. Ikeda, N. Hirata, Y. Moriya, M. Kubo, O. Yamamoto, J. Power Sources 81–82 (1999) 824–829.
[29] P. Majsztrik, A. Bocarsly, J. Benziger, J. Phys. Chem. B 112 (2008) 16280–16289.
[30] E. Tsuchida, H. Ohno, K. Tsunemi, Electrochim. Acta 28 (1983) 833–837.
[31] R. Jiang, T. Huang, Y. Tang, J. Liu, L. Xue, J. Zhuang, A. Yu, Electrochim. Acta 54 (2009) 7173–7179.
[32] P. Sivaraman, S.K. Rath, V.R. Hande, A.P. Thakur, M. Patri, A.B. Samui, J. Power Sources 156 (2006) 1057–1064.
[33] B.E. Conway, Electrochemical Supercapacitors, Scientific Fundamentals and Technological Application, Kluwer Academic/Planum, New York, 1999.
[34] Y.G. Wang, X.G. Zhang, Solid State Ionics 166 (2004) 61–67.
[35] F. Lufrano, P. Staiti, Electrochim. Acta 49 (2004) 2683–2689.
[36] J. Lee, Y. Lee, W. Chae, Y. Sung, J. Electroceram. 17 (2006) 941–944.
[37] T. Ikeshoji, J. Electroanal. Chem. 296 (1990) 19–36.
[38] A.B. Fuertes, G. Lota, T.A. Centeno, E. Frackowiak, Electrochim. Acta 50 (2005) 2799–2805.
[39] W. Sun, X. Chen, J. Power Sources 193 (2009) 924–929.